



CrossMark
click for updates

Cite this: *RSC Adv.*, 2016, 6, 110928

Fe₃O₄@PEG-SO₃H rod-like morphology along with the spherical nanoparticles: novel green nanocomposite design, preparation, characterization and catalytic application†

Ali Maleki,* Pedram Zand and Zahra Mohseni

The design and preparation of polyethylene glycol sulfonic acid surface coated magnetic nanoparticles (Fe₃O₄@PEG-SO₃H) is described. The morphology of the prepared nanocomposite was rod-like along with spherical nanoparticles. It was characterized by Fourier transform infrared (FT-IR) spectroscopy, field-emission scanning electron microscopy (FE-SEM), X-ray diffraction (XRD), energy-dispersive X-ray (EDX), vibrating sample magnetometry (VSM), N₂ adsorption-desorption by Brunauer-Emmett-Teller (BET) and inductively coupled plasma (ICP) analysis. Furthermore, this novel heterogeneous catalyst was successfully used in a multicomponent one-pot reaction for the synthesis of dihydropyrimidine derivatives. This efficient protocol includes some other advantages such as using ethanol as a green solvent, no significant decrease in the activity of the nanocatalyst during the recovery process, relatively short reaction times and high-to-excellent yields of the products.

Received 27th September 2016
Accepted 16th November 2016

DOI: 10.1039/c6ra24029a

www.rsc.org/advances

Introduction

Recently, due to importance of catalysts and catalytic reactions in chemical research and industry, the catalytic performances of heterogeneous catalysts compared to their counterpart homogeneous ones have been widely improved by bringing the catalysts to the nanoscale to provide higher surface area and enhance the contact frequency between them and the reaction components.¹⁻⁴ Supported magnetic nanoparticles (MNPs) are important in the field of green chemistry. MNPs are typically surface-modified or coated with biocompatible polymers which improve their colloidal stability in physiological media and reduce toxicity. MNPs have found various applications in different disciplines such as biomedicine, catalysis, bioseparation, data storage, magnetic resonance imaging, *etc.* Fe₃O₄ nanoparticles are attractive because of their low cost, reactive surfaces, high specific surface area and easy separation. Recently, a few functionalized Fe₃O₄ MNPs have been employed in a wide variety of organic reactions.^{5,6}

Polyethylene glycol (PEG) is an important biocompatible synthetic polymer that could be used as a coating agent for nanoparticles. Due to its unique properties such as extremely hydrophilic nature (hydrophilicity), flexibility, non-toxicity and nonimmunogenicity,⁷ the introduction of any new protocol for

the synthesis of PEG-coated MNPs is of prime importance. Although, a few strategies have been reported in the literature for the modification of PEG-based MNPs, the synthetic pathway was remained almost complicated up to now. In other words, most of them suffer from harsh reaction conditions.⁸ For example, in a typical work, refluxing temperature (above 200 °C) has been applied for the synthesis of PEG-coated MNPs.⁹

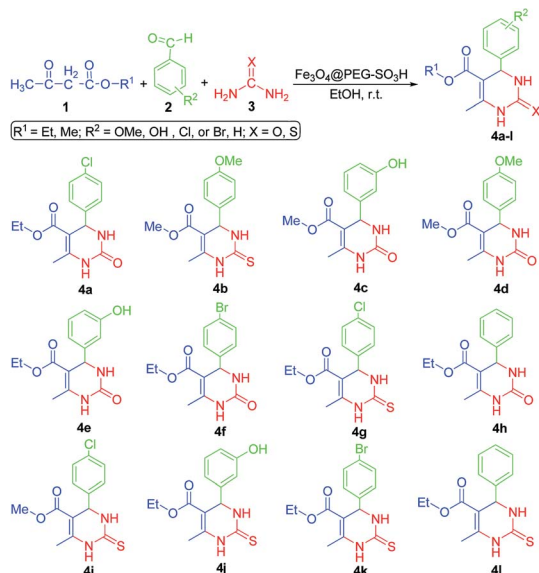
Dihydropyrimidines (DHPMs) are well-known scaffolds that are easily prepared through the condensation reaction of urea/thiourea, β-ketoesters and aryl aldehydes.¹⁰ DHPMs have a significant role in medicinal chemistry because of their various pharmacological activities such as anticancer, antibacterial, antifungal, antihypertensive, antitubercular, antimalarial, antiviral and anti-inflammatory.¹¹⁻¹³ Therefore, design and development of inexpensive, general, and reusable catalysts in conjunction with multicomponent reactions strategy for the synthesis of DHPMs is of prime importance.

In continuation of our research on the introduction of new recoverable nanocatalysts and their applications in organic synthesis,¹⁴⁻¹⁸ herein, we wish to report a convenient and facile multicomponent one-pot synthesis of DHPMs **4a-I** via the condensation of β-ketoesters **1**, aldehydes **2** and urea or thiourea **3** in the presence of Fe₃O₄@PEG-SO₃H as a superparamagnetic heterogeneous nanocatalyst (Scheme 1).

To the best of our knowledge, this is the first report on design, preparation and characterization of Fe₃O₄@PEG-SO₃H nanocomposite and its application as a novel, efficient, eco-friendly catalyst in chemical reactions, especially in organic synthesis such as DHPMs. Furthermore, the surface modification procedure

Catalysts and Organic Synthesis Research Laboratory, Department of Chemistry, Iran University of Science and Technology, Tehran 16846-13114, Iran. E-mail: maleki@iust.ac.ir; Fax: +98 21 73021584; Tel: +98 21 77240540

† Electronic supplementary information (ESI) available. See DOI: 10.1039/c6ra24029a



Scheme 1 $\text{Fe}_3\text{O}_4@\text{PEG-SO}_3\text{H}$ catalyzed synthesis of DHPMs 4a–l.

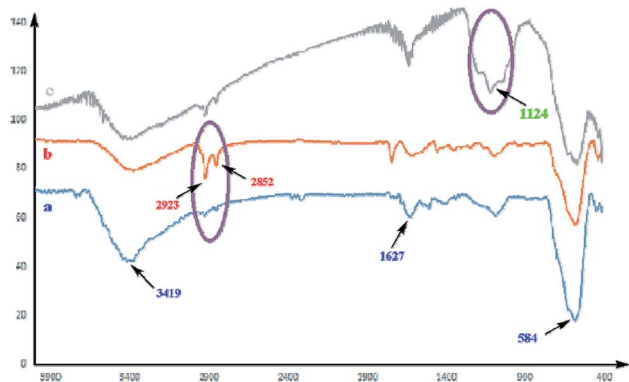


Fig. 1 The comparative FT-IR spectra of: (a) Fe_3O_4 , (b) $\text{Fe}_3\text{O}_4@\text{PEG}$ and (c) $\text{Fe}_3\text{O}_4@\text{PEG-SO}_3\text{H}$.

described in this work can be classified as a green protocol because of using water and ethanol as solvents, room temperature reactions, and safe and simple reaction conditions.

Results and discussion

Characterization of the prepared $\text{Fe}_3\text{O}_4@\text{PEG-SO}_3\text{H}$ nanocatalyst

$\text{Fe}_3\text{O}_4@\text{PEG-SO}_3\text{H}$ nanocatalyst was prepared by *in situ* co-precipitation method. As can be seen in Fig. 1, the FT-IR spectrum of the $\text{Fe}_3\text{O}_4@\text{PEG-SO}_3\text{H}$ magnetic nanocatalyst can verify the preparation of the expected product. The bending vibration band at 584 cm^{-1} and stretching vibration band at 1627 cm^{-1} is induced by structure Fe–O vibration. A broad O–H stretch around 3419 cm^{-1} was observed in both Fe_3O_4 and the PEG coated MNPs. The C–H stretching vibrations observed at 2852 and 2923 cm^{-1} indicate that the PEG was successfully composed onto the surfaces of Fe_3O_4 nanoparticles. The functionalization of SO_3H groups on $\text{Fe}_3\text{O}_4@\text{PEG}$ surface was approved by the absorption band at 1124 cm^{-1} of the S=O stretching vibrations.

To clarify the morphology of the nanocatalyst, FE-SEM images of $\text{Fe}_3\text{O}_4@\text{PEG-SO}_3\text{H}$ were provided (Fig. 2). It can be seen that the nanocatalyst was uniformly prepared and the main structure of nanocatalyst was rod-like morphology along with the spherical iron oxide (II, III) nanoparticles. In addition, the nanosized structure and morphology of the catalyst was proved by FE-SEM images.

The result of the EDX analysis of the $\text{Fe}_3\text{O}_4@\text{PEG-SO}_3\text{H}$ magnetic nanoparticles was illustrated in Fig. 3. It confirms the presence of carbon, oxygen and sulfur elements in the nanocatalyst.

Fig. 4 shows the XRD measurements were performed with the dried powder samples of bare and PEG coated MNPs to identify the crystal phases present in the samples. The XRD pattern of a representative $\text{Fe}_3\text{O}_4@\text{PEG-SO}_3\text{H}$ (curve a) along with bare Fe_3O_4 NPs (curve b). The pattern of the $\text{Fe}_3\text{O}_4@\text{PEG-SO}_3\text{H}$ showed all the major peaks corresponding to Fe_3O_4 . The diffraction angles (2θ) of 30.28 , 35.64 , 43.28 , 57.24 , 62.87 and 74.42 can be assigned to $2\ 2\ 0$, $3\ 1\ 1$, $4\ 0\ 0$, $5\ 1\ 1$, $4\ 4\ 0$, and $5\ 3\ 3$ planes, respectively; which are in accordance with Fe_3O_4 reference pattern (JCPDS#19-0629). Additionally, one peak around $2\theta = 25^\circ$ along with small peaks due to the PEG- SO_3H polymer are observed in the case of the $\text{Fe}_3\text{O}_4@\text{PEG-SO}_3\text{H}$. These results

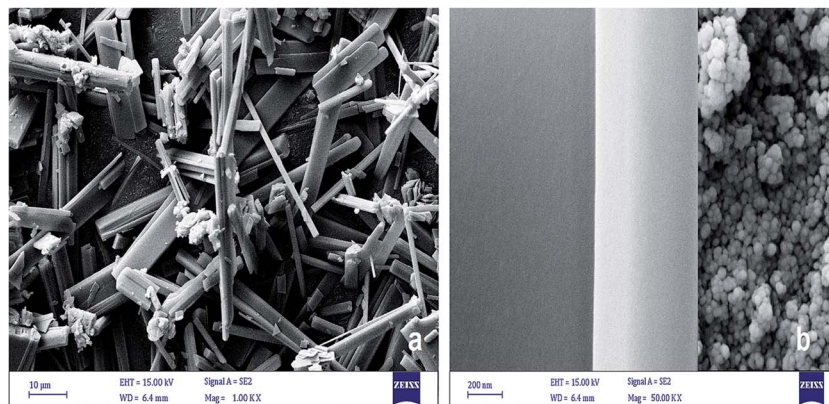


Fig. 2 FE-SEM images of $\text{Fe}_3\text{O}_4@\text{PEG-SO}_3\text{H}$ rod-like nanocatalyst with different magnifications: (a) $10\ \mu\text{m}$ and (b) $200\ \text{nm}$.

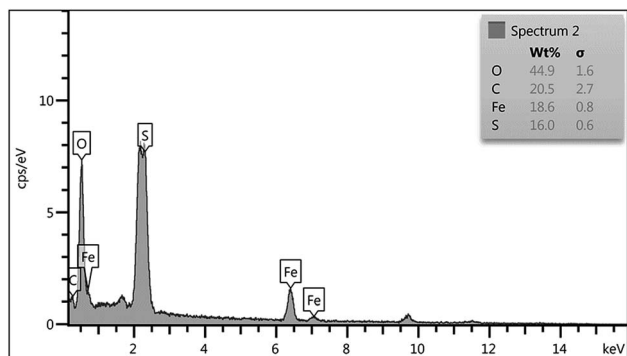


Fig. 3 EDX analysis of Fe_3O_4 @PEG- SO_3H nanocatalyst.

confirmed the surface modification of the Fe_3O_4 NPs with PEG- SO_3H .

The magnetic properties of Fe_3O_4 , Fe_3O_4 @PEG and Fe_3O_4 @PEG- SO_3H were measured by VSM curves at room temperature. As can be seen in Fig. 5, the hysteresis loops of the superparamagnetic behavior can be clearly observed for all the nanoparticles. The superparamagnetism is responsible to an applied magnetic field without retaining any magnetism after removal of the applied magnetic field. From M versus H curves, the saturation magnetization value (M_s) of uncoated MNPs was found to be 56 emu g^{-1} . For Fe_3O_4 @PEG and Fe_3O_4 @PEG- SO_3H the magnetizations obtained at the same field were 38 and 27 emu g^{-1} , respectively, those were lower than neat Fe_3O_4 nanoparticles. This is mainly attributed to the existence of materials on the surface of the nanoparticles. The photograph of the magnetic separation of catalyst from the organic reactions mixture was shown in Fig. 5.

Furthermore, inductively coupled plasma (ICP) analyses of the catalysts revealed that the metal (Fe) content of the catalyst ($\pm 0.4\%$) were close to target metal content (12.24 wt%).

The specific surface area of Fe_3O_4 @PEG- SO_3H was measured by using Brunauer-Emmett-Teller (BET) analysis with N_2 adsorption-desorption. BET surface area of Fe_3O_4 @PEG- SO_3H was $43.86 \text{ m}^2 \text{ g}^{-1}$. The reduced amount of surface area in comparison with iron oxide (II, III) nanoparticles may be the

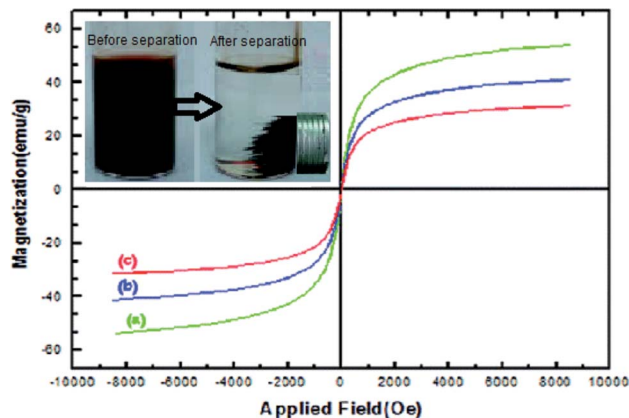


Fig. 5 VSM magnetization curves of: (a) Fe_3O_4 , (b) Fe_3O_4 @PEG and (c) Fe_3O_4 @PEG- SO_3H .

consequence/confirmation of immobilization of PEG- SO_3H on Fe_3O_4 nanoparticles.

Catalytic application of Fe_3O_4 @PEG- SO_3H in the synthesis of DHPMs

Initially, to optimize the reaction conditions for the synthesis of DHPMs, various parameters were studied on the reaction of β -

Table 1 Optimizing of the reaction conditions

Entry	Nano- Fe_3O_4 @PEG- SO_3H (g)	Solvent	Time (min)	Yield (%)
1	0.005	EtOH	70	70
2	0.010	EtOH	20	95
3	0.015	EtOH	100	75
4	0.020	EtOH	110	60
5	0.010	MeOH	125	65
6	0.010	H_2O	90	40
7	0.010	MeCN	130	43
8	0.010	DMF	100	55
9	0.010	Solvent-free	90	35

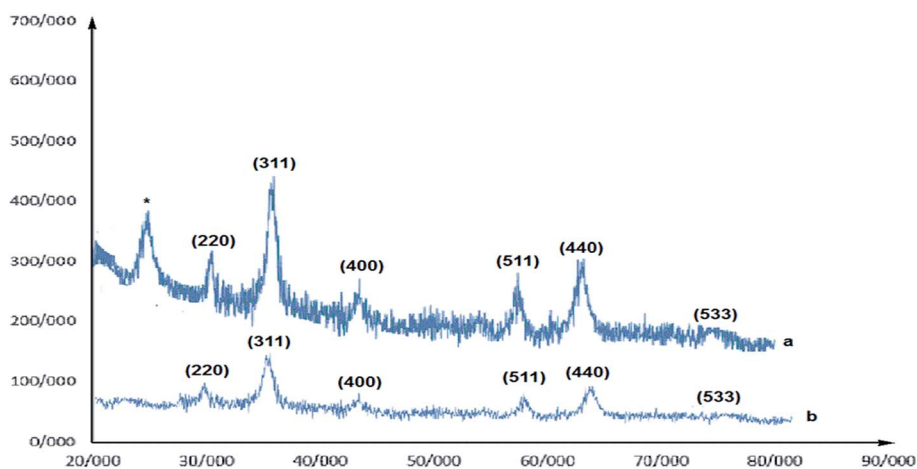


Fig. 4 The XRD pattern of: (a) Fe_3O_4 @PEG- SO_3H and (b) Fe_3O_4 . The symbol "*" represents the PEG- SO_3H peak.

Table 2 A comparison of some catalysts effects with the present nanocatalyst on the model reaction

Entry	Catalyst	Temperature (°C)	Time	Yield (%)	Ref.
1	Nano-Fe ₃ O ₄ @PEG-SO ₃ H	r.t.	20 min	95	This work
2	Nano-Fe ₃ O ₄ @PEG	r.t.	45 min	90	This work
3	Nano-Fe ₃ O ₄	r.t.	50 min	85	This work
4	PEG-SO ₃ H	r.t.	60 min	80	This work
5	PEG	r.t.	48 h	75	This work
6	—	100	8 h	15	This work
7	Montmorillonite KSF	130	48 h	77	19
8	Silica-sulfuric acid	Reflux	6 h	91	20
9	H ₃ PMo ₁₂ O ₄₀	Reflux	5 h	80	21
10	ZrOCl ₂ ·8H ₂ O	100	2 h	56	22

diketone (2 mmol), aromatic aldehyde (2 mmol) and urea or thiourea (2.4 mmol), as a pilot test. First, the effect of the catalyst amount on the reaction yield was studied. It was found that using 0.010 g of the Fe₃O₄@PEG-SO₃H nanocatalyst is sufficient to complete the reaction and give **4a** after 20 min in 95% yield in 4 mL of EtOH as a green solvent at room temperature. The results summarized in Table 1. To compare the efficiency of ethanol, several solvents with different polarities were tested using the model reaction in the presence Fe₃O₄@PEG-SO₃H. As it obvious from the results, it was found that ethanol is the superior solvent for this study than MeOH, H₂O, MeCN and DMF in the presence of 0.010 g of Fe₃O₄@PEG-SO₃H catalyst at room temperature.

Finally, a comparison was done between the present work and others earlier reports for the synthesis of **4a**. The results summarized in Table 2 clearly demonstrate the superiority of the present work in saving energy, high yields of the products and the reusability of the nanocatalyst.

In order to investigate the scope and limitations of the present protocol and to show the application of Fe₃O₄@PEG-SO₃H in the synthesis of DHPMs, a variety of products were synthesized under the optimized conditions. The results summarized in Table 3 shows that all products were obtained in good-to-excellent yields after appropriate reaction times. The

Table 4 Calculated values of turnover number (TON) and turnover frequency (TOF) for DHPMs

Entry	Product	TON	TOF/h ⁻¹
1	4a	67.857	3.392
2	4b	57.142	0.816
3	4c	60	1.333
4	4d	57.142	0.952
5	4e	60	1.333
6	4f	65.714	1.877
7	4g	67.857	2.261
8	4h	60.714	1.214
9	4i	65.714	1.194
10	4j	63.571	1.558
11	4k	64.285	1.607
12	4l	60.714	1.103

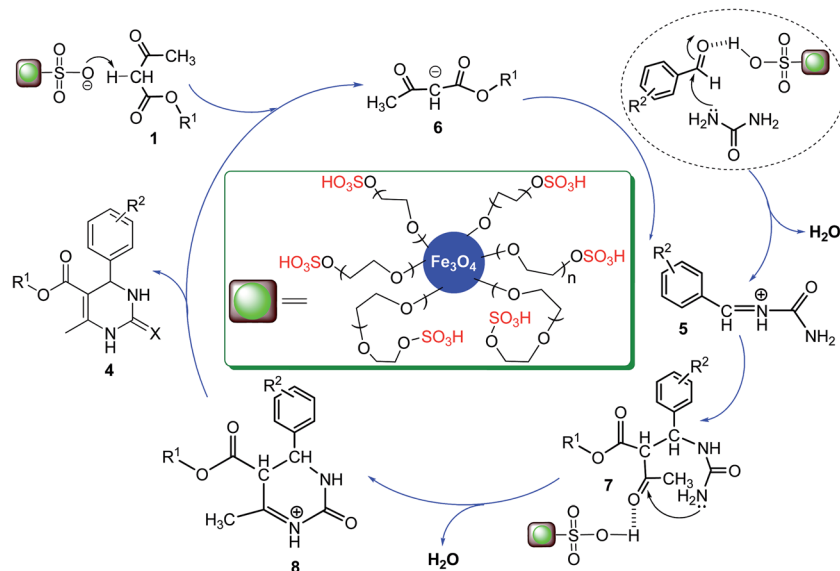
corresponding reaction yields, TON and TOF values are also listed in Table 4.

The suggested possible mechanism for the formation of DHPMs **4a–l** is shown in Scheme 2. On the basis of the literature and substrates chemistry, the first step is believed to be the condensation between an aldehyde and urea or thiourea in the presence of Fe₃O₄@PEG-SO₃H, similar to the

Table 3 Synthesis of DHPMs **4a–l** by using Fe₃O₄@PEG-SO₃H nanocatalyst

Entry	R ¹	R ²	X	Product	Time (min)	Yield ^a (%)	Mp (°C)	
							Found	Reported
1	Et	4-Cl	O	4a	20	95	213	212–214 (ref. 23)
2	Me	4-OMe	S	4b	70	80	153	153–155 (ref. 24)
3	Me	3-OH	O	4c	45	84	222	220–222 (ref. 25)
4	Me	4-OMe	O	4d	60	80	195	194–195 (ref. 26)
5	Et	3-OH	O	4e	45	84	221	221–222 (ref. 27)
6	Et	4-Br	O	4f	35	92	213	213–214 (ref. 28)
7	Et	4-Cl	S	4g	30	95	180	179–180 (ref. 29)
8	Et	H	O	4h	50	85	201	201–203 (ref. 30)
9	Me	4-Cl	S	4i	30	92	243	241–243 (ref. 31)
10	Et	3-OH	S	4j	55	84	182	181–185 (ref. 32)
11	Et	4-Br	S	4k	40	90	180	178–180 (ref. 33)
12	Et	H	S	4l	55	85	203	204–206 (ref. 34)

^a Isolated yield.



Scheme 2 The proposed mechanism for the formation of DHPMs in the presence of $\text{Fe}_3\text{O}_4@$ PEG- SO_3H nanocatalyst.

Mannich condensation reaction. The produced iminium 5 acts as an electrophile for the nucleophilic addition of the ketoester carbanion 6 (obtained from 1 attached by anion form of the nanocatalyst) to yield intermediate 7. Then, the carbonyl group of ketone of the resulting adduct undergoes condensation with the NH_2 of urea part to give the compound 8. Finally, an imine–enamine tautomerization of 8 leads to the formation of the products 4.¹⁰

Recyclability of $\text{Fe}_3\text{O}_4@$ PEG- SO_3H nanocatalyst

The reusability of $\text{Fe}_3\text{O}_4@$ PEG- SO_3H catalyst was studied in the model reaction. In this regard, after completion of the reaction, the nanocatalyst were separated by an external magnet and washed with ethanol and water, dried and reused in subsequent reactions. It was observed that the catalyst can be reused at least six times without any significant decrease in yield of the products (Fig. 6).

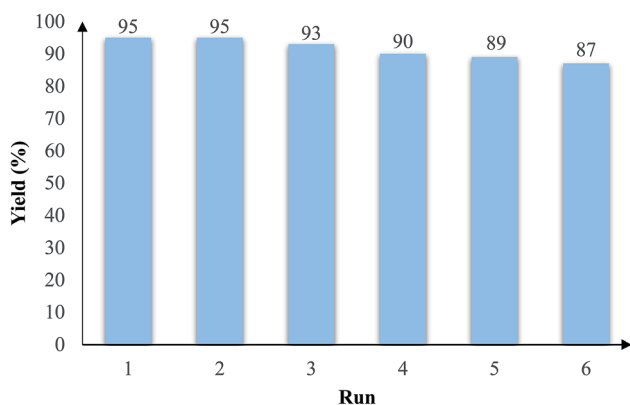


Fig. 6 Recycling of $\text{Fe}_3\text{O}_4@$ PEG- SO_3H nanocatalyst in the synthesis of 4a.

Conclusions

In summary, $\text{Fe}_3\text{O}_4@$ PEG- SO_3H as a novel, highly efficient, simple, green and cost-effective, environmentally-friendly and reusable superparamagnetic nanocatalyst was described. It was prepared through a facile process and completely characterized by FT-IR spectroscopy, FE-SEM images, XRD pattern, EDX, VSM, BET and ICP analyses. Then, the catalytic property of the nanocomposite was investigated in the synthesis of DHPMs. The products were obtained in high-to-excellent yields at room temperature under simple reaction conditions. The nanocatalyst was easily recovered by an external magnet and reused efficiently for the several runs without significant decrease in activity. This is the first report on design, *in situ* synthesis, functionalization and characterization of the present nanocomposite and also performance as a heterogeneous catalyst in organic reactions.

Experimental

General

All the solvents, chemicals and reagents were purchased from Merck, Sigma and Aldrich. Melting points were measured on an Electrothermal 9100 apparatus and are uncorrected. Fourier transforms infrared spectroscopy (FT-IR) spectra were recorded on a Shimadzu IR-470 spectrometer by the method of KBr pellet. ^1H and ^{13}C NMR spectra were recorded on a Bruker DRX-300 Avance spectrometer at 300 and 75 MHz, respectively. Field-emission scanning electron micrograph (FE-SEM) images were taken with Sigma-Zeiss microscope with attached camera. Magnetic measurements of the solid samples were performed using Lakeshore 7407 and Meghnatis Kavir Kashan Co., Iran vibrating sample magnetometers (VSMs). Elemental analysis of the nanocatalyst was carried out by energy-dispersive X-ray (EDX) analysis recorded Numerix DXP-X10P. X-ray diffraction patterns of the solid powders

were recorded with a X' Pert Pro X-ray diffractometer operating at 40 mA, 40 kV. The specific surface area was measured *via* BET N₂ adsorption–desorption method by using a Nansord92 instrument. Inductively coupled plasma (ICP) analysis was provided on a Shimadzu ICPS-7000.

Preparation of Fe₃O₄@PEG nanoparticles

Fe₃O₄@PEG nanoparticles were prepared *via in situ* co-precipitation method. In a typical procedure, 2.4 g FeCl₃ and 3.0 g FeCl₂·5H₂O in 100 mL of deionized water to be solved. Then, 40 mL of PEG-400 was mixed with 10 mL of NH₃·H₂O at 30 °C in a three-necked flask. Then, the mixture of FeCl₃ and FeCl₂·5H₂O was slowly added in NH₃-PEG solution during 150 min at 30 °C. The obtained Fe₃O₄/PEG precipitate was washed with deionized water until pH was reached to 7. Finally, it was dried at 80 °C in an oven.

Preparation of Fe₃O₄@PEG-SO₃H nanoparticles

A 500 mL suction flask was equipped with a constant pressure dropping funnel. The gas outlet was connected to a vacuum system through an adsorbing solution of alkali trap. Fe₃O₄@PEG (2.0 g) was added to the flask and dispersed by an ultrasonic bath for 10 min in CH₂Cl₂ (75 mL). Then, a solution of chlorosulfonic acid (1 mL) in CH₂Cl₂ (20 mL) was added dropwise over a period of 30 min at 0 °C. After completion of the addition, the mixture was shaken for 90 min, to remove residual HCl. After that, Fe₃O₄@PEG-SO₃H was separated from the reaction mixture by a magnetic bar and washed several times with dry CH₂Cl₂. Finally, Fe₃O₄@PEG-SO₃H was dried under vacuum at 60 °C.

General procedure for the synthesis of DHPMs 4a–I

A mixture of an aromatic aldehyde (2.0 mmol), β-ketoester (2.0 mmol), urea or thiourea (2.4 mmol) and Fe₃O₄@PEG-SO₃H (0.01 g) in absolute EtOH (4 mL) was stirred at room temperature. The completion of the reaction was monitored by thin layer chromatography (TLC). After completion of the reaction, the catalyst was separated easily by an external magnet. The pure products were obtained from the reaction mixture by recrystallization from hot EtOH and no more purification was required.

Spectral data of ethyl 4-(4-chlorophenyl)-1,2,3,4-tetrahydro-6-methyl-2-oxypyrimidine-5-carboxylate 4a

White crystalline solid: mp 212–214 °C. FT-IR (KBr) (ν_{\max} , cm⁻¹): 852, 1091, 1222, 1598, 1649, 17 026, 2977, 3114, 3303. ¹H NMR (300 MHz, DMSO-*d*₆) (δ , ppm): 1.13–1.19 (t, 3H, CH₃), 1.78 (s, 3H, CH₃), 4.19 (m, 2H, CH₂), 5.75 (s, 1H, CH), 6.00 (m, 2H, NH), 7.00 (d, 2H, H-Ar), 7.15 (d, 2H, H-Ar). ¹³C NMR (75 MHz, DMSO-*d*₆) (δ , ppm): 14.2, 14.9, 49.5, 61.7, 106.4, 128.4, 128.9, 132.3, 141.3, 174.3, 150.4, 167.2.

Acknowledgements

The authors gratefully acknowledge the partial support from the Research Council of the Iran University of Science and Technology.

References

- (a) P. T. Anastas and M. M. Kirchhoff, *Acc. Chem. Res.*, 2002, **35**, 686–694; (b) G. G. Kumar, C. J. Kirubaharan, A. R. Kim and D. J. Yoo, *Ind. Eng. Chem. Res.*, 2012, **51**, 15625–15632; (c) S. Li, Y. Li, X. Zeng, W. Wang, R. Shi and L. Ma, *RSC Adv.*, 2015, **5**, 68700–68713.
- (a) R. H. Vekariya, K. D. Patel and H. D. Patel, *RSC Adv.*, 2015, **5**, 90819–90837; (b) L. Cabrita, V. Petrov and F. Pian, *RSC Adv.*, 2014, **4**, 18939–18944.
- V. Polshettiwar, R. Luque, A. Fihri, H. Zhu, M. Bouhrara and J. M. Basset, *Chem. Rev.*, 2011, **111**, 3036–3075.
- S. Shylesh, V. Schünemann and W. R. Thiel, *Angew. Chem., Int. Ed.*, 2010, **49**, 3428–3459.
- N. Jain, J. Xu, R. M. Kanojia, F. Du, G. Jian-Zhong, E. Pacia, M. T. Lai, A. Musto, G. Allan and M. Reuman, *J. Med. Chem.*, 2009, **52**, 7544–7569.
- (a) L. Douziech-Eyrolles, H. Marchais and K. Herve, *Int. J. Nanomed.*, 2007, **2**, 541–550; (b) M. Vinothkannan, C. Karthikeyan, G. G. Kumar, A. R. Kim and D. J. Yoo, *Spectrochim. Acta, Part A*, 2015, **136**, 256–264; (c) J. Salamon, Y. Sathishkumar, K. Ramachandran, Y. S. Lee, D. J. Yoo, A. R. Kim and G. G. Kumar, *Biosens. Bioelectron.*, 2015, **64**, 269–276; (d) M. Ranjani, Y. Sathishkumar, Y. S. Lee, D. J. Yoo, A. R. Kim and G. G. Kumar, *RSC Adv.*, 2015, **5**, 57804–57814; (e) G. G. Kumar, Z. Awan, K. S. Nahm and J. S. Xavier, *Biosens. Bioelectron.*, 2014, **53**, 528–534.
- J. F. Lutz, S. Stoller, A. Hoth, L. Kaufner, U. Pison and R. Cartier, *Biomacromolecules*, 2006, **7**, 3132–3138.
- J. Y. Park, D. Patel, G. H. Lee, S. Woo and Y. Chang, *Nanotechnology*, 2008, **19**, 365603–365609.
- (a) J. Amici, A. Allia, P. Tiberto and M. Sangermano, *Macromol. Chem. Phys.*, 2011, **212**, 1629–1635; (b) G. G. Kumar, C. J. Kirubaharan, S. Udhayakumar, C. Karthikeyan and K. S. Nahm, *Ind. Eng. Chem. Res.*, 2014, **53**, 16883–16893; (c) T. R. Kumar, K. J. Babu, D. J. Yoo, A. R. Kim and G. G. Kumar, *RSC Adv.*, 2015, **5**, 41457–41467.
- (a) C. O. Kappe, *Acc. Chem. Res.*, 2000, **12**, 879–888; (b) M. Michalak, M. Kwiecień, M. Kawaleca and P. Kurcok, *RSC Adv.*, 2016, **6**, 12809–12818; (c) N. Senthilkumar, K. Justice Babu, G. Gnanakumar, A. R. Kim and D. J. Yoo, *Ind. Eng. Chem. Res.*, 2014, **53**, 10347–10357.
- R. Mishra and I. Tomar, *Int. J. Pharm. Sci. Res.*, 2011, **2**, 758–771.
- (a) B. Sedaghati, A. Fassihi, S. Arbabi, M. Ranjbar, L. Saghaie and A. Sardari, *Med. Chem. Res.*, 2012, **21**, 3973–3983; (b) G. G. Kumar, C. Joseph Kirubaharan, S. Udhayakumar, K. Ramachandran, C. Karthikeyan, R. Renganathan and K. S. Naham, *ACS Sustainable Chem. Eng.*, 2014, **2**, 2283–2290; (c) P. H. Secrétan, H. S. Yayé, C. A. Chodur,

- M. Bernard, A. Solgadi, F. Amrani, N. Yagoubi and B. Do, *RSC Adv.*, 2015, **5**, 35586–37797; (d) G. G. Kumar, K. Justice Babu, K. S. Naham and Y. J. Hwang, *RSC Adv.*, 2014, **4**, 7944–7951; (e) G. G. Kumar, S. Hashmi, C. Karthikeyan, A. Ghavaminenejad, M. Vatankhah Varnoosfaderani and F. J. Stadler, *Macromol. Rapid Commun.*, 2014, **35**, 1861–1865; (f) C. Joseph Kirubaharan, K. Santhakumar, G. G. Kumar, N. Senthilkumar and J. H. Jang, *Int. J. Hydrogen Energy*, 2015, **40**, 13061–13070.
- 13 R. H. Tale, A. H. Rodge, G. D. Hatnapure, A. P. Keche, K. M. Patil and R. P. Pawar, *Med. Chem. Res.*, 2012, **21**, 4252–4260.
- 14 A. Maleki, *Tetrahedron*, 2012, **68**, 7827–7833.
- 15 A. Maleki, *Tetrahedron Lett.*, 2013, **54**, 2055–2059.
- 16 A. Maleki, *RSC Adv.*, 2014, **4**, 64169–64173.
- 17 A. Maleki and M. Kamalzare, *Catal. Commun.*, 2014, **53**, 67–71.
- 18 A. Maleki and R. Paydar, *RSC Adv.*, 2015, **5**, 33177–33184.
- 19 F. Bigi, S. Carloni, B. Frullanti, R. Maggi and G. Sartori, *Tetrahedron Lett.*, 1999, **40**, 3465–3468.
- 20 P. Salehi, M. Dabiri, M. A. Zolfigol and M. A. Bodaghifard, *Tetrahedron Lett.*, 2003, **44**, 2889–2891.
- 21 M. M. Heravi, K. Bakhtiari and F. F. Bamoharram, *Catal. Commun.*, 2006, **7**, 373–376.
- 22 J. C. Rodriguez-Dominguez, D. Bernardi and G. Kirsch, *Tetrahedron Lett.*, 2007, **48**, 5777–5780.
- 23 Z. Abdolkarim and Z. Nasouri, *J. Mol. Liq.*, 2016, **216**, 364–369.
- 24 S. R. Jetti, A. Upadhyaya and S. Jain, *Med. Chem. Res.*, 2014, **23**, 4356–4366.
- 25 C. Mukhopadhyay and A. Datta, *J. Heterocycl. Chem.*, 2010, **47**, 136–146.
- 26 L. Saher, M. Makhloufi-Chebli, L. Dermeche, B. Boutemeur-Khedis, C. Rabia, A. M. S. Silva and M. Hamdi, *Tetrahedron Lett.*, 2016, **57**, 1492–1496.
- 27 S. Nagarajan, T. M. Shaikh and E. Kandasamy, *J. Chem. Sci.*, 2015, **127**, 1539–1545.
- 28 J. Javidi, M. Esmaeilpour and F. Dodeji, *Eur. J. Org. Chem.*, 2015, 6994–6998.
- 29 J. Javidi, M. Esmaeilpour and F. Dodeji, *RSC Adv.*, 2015, **5**, 308–315.
- 30 S. R. Jetti, A. Bhatewara, T. Kadre and S. Jain, *Chin. Chem. Lett.*, 2014, **25**, 469–473.
- 31 M. Nasr-Esfahani, M. Montazerzohori, M. Aghel-Mirrezaee and H. Kashi, *J. Chil. Chem. Soc.*, 2014, **59**, 2311–2314.
- 32 N. A. Al-Masoudi, N. J. Al-Salihi, Y. A. Marich and T. Markus, *J. Fluoresc.*, 2016, **26**, 31–35.
- 33 P. K. Sahoo, A. Bose and P. Mal, *Eur. J. Org. Chem.*, 2015, 6994–6998.
- 34 R. Rezaei, M. K. Mohammadi and A. Khaledi, *Asian J. Chem.*, 2013, **25**, 4588–4590.